Cortical Mapping of EEG Alpha Power Using a Charge Layer Model

Dezhong Yao*+, Li Wang*, Kim Dremstrup Nielsen*, Lars Arendt-Nielsen*, and Andrew C.N. Chen*

Summary: This study aims to investigate how the blurred scalp alpha power distribution can be segregated on the cortex. EEG recorded from 11 subjects with their eyes closed were utilized to reconstruct the cortically equivalent Charge Layer (CL). Further, the power maps of scalp potential as well CL were generated by Fourier transform. The results showed a distinctly different CL power distribution from that of the scalp potential power, the cortical alpha electric activities were separated significantly into the left and right occipital regions, and in some cases activities at parietal regions were also clearly visibly discriminated. We concluded that the CL model is sensitive, and the blurred scalp activities can be further delineated into separate regions.

Key words: Alpha; Electroencephalography; Charge layer; EEG mapping; Cortical differentiation.

Introduction

Spontaneous EEG phenomena represent endogenous patterns of neural activity and are of interest both scientifically and clinically. Questions whether spontaneous EEG rhythm, such as alpha, arise from anatomically distinct networks (Niedermeyer 1997; Klimesch et al. 1998), or is a consequence of global dynamics (Lopes da Silva et al. 1997) are important with fundamental implications for understanding higher order cognitive processes. In this study, we addressed the alpha rhythm oscillating around 10Hz. It is the dominant rhythm in the human scalp EEG of relaxed but alert adults while the eyes are closed, largely disappearing when the eyes are open. Initially, Hans Berger (Berger 1929) described that the alpha rhythm has been regarded as representing a resting or "idling" state of the underlying cortex (Adrian and Matthews 1934). This is now giving way to views that relate with diverse brain functions comprising sensory, motor, and memory processes (Basar et al. 1997).

Regarding source models of alpha rhythms, several authors (Lu et al. 1992; Salenius et al. 1995; Michel et al. 1992; Tesche and Kajola 1993) reported dipole sources predominantly located in the parieto-occipital area with additional dipoles located around the calcarine fissure (Salenius et al.1995; Williamson and Kaufman 1989; Parra et al. 2000) and left parietal occipital sulcus (Tesche et al. 1995). There are also reported alpha sources localized near the mid-line in the basal portions of the occipital lobe (Rodin 1995). These results suggested that the alpha activity has multiple generators (Basar et al. 1997) with some being more active than others in a concrete case. In fact, with intra-cranial electrodes in the human brain, alpha rhythms could be traced throughout the whole occipital cortex (Perez-Borja et al. 1962). Therefore, rather than trying to locate a unique alpha generator, it is preferable to assume the existence of a "diffuse and distributed alpha system" (Basar et al. 1997). These facts motivated the use of a distributed source model in localizing spontaneous human brain activity including the alpha rhythm (Tesche et al. 1995; Patel et al. 1999; Narici and Romani 1989). All subjects in a study showed the alpha activities primarily distributed over the occipital and parieto-occipital areas, and most of the subjects showed bilateral distribution of the dipole sources (Patel et al. 1999).

* Human Brain Mapping and Cortical Imaging Laboratory, Centre for Sensory Motor Interaction, Aalborg University, Aalborg, Denmark.

+ School of Life Science and Technology, University of Electronic Science and Technology of China, Chengdu, China.

Accepted for publication: November 5, 2004.

This work is supported by funding from the Danish National Research Foundation, the International Centre for Biomedical Research of Denmark, Aalborg University Visiting Scientists Award, and the NSFC.90208003 and the 973 Project No. 2003CB716106 (D. Yao), Doctor Training Fund of MOE, Key research project of science and technology of MOE, and TRAPOYT. Thanks to Dr. Robert Oostenveld for his comments on the first version, and the reviewers for their comments on the previous version.

Correspondence and reprint requests should be addressed to Dezhong Yao, School of Life Science and Technology, University of Electronic Science and Technology of China, Chengdu 610054, China.

Tel/Fax: 86-28-83206124.

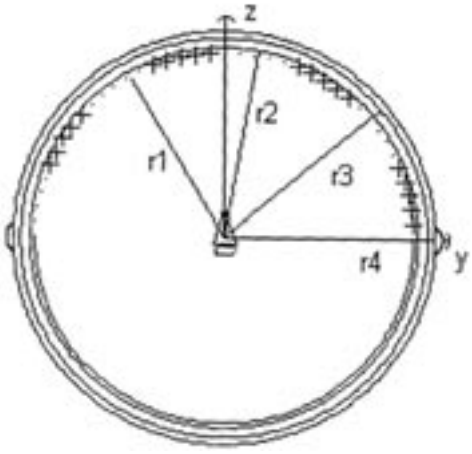

Figure 1. Concentric four-sphere Conductor head model and equivalent charge layer. In this model, the radii are r1=7.9cm, r2=8.1cm, r3=8.5cm and r4= 8.8cm for the outer boundaries of the inner brain sphere, the cerebrospinal fluid layer, the skull layer, and the scalp layer, respectively. And the conductivities are 0.461 A/(Vm), 1.39 A/(Vm), 0.0058 A/(Vm), and 0.461 A/(Vm), respectively. The discrete equivalent charge layer is on the upper hemisphere with r_T =7.5cm where the sum of positive (+) and negative (.) charges are zero.

About the equivalent charge (monopole) source models of neural electric activities (Malmivuo and Plonsey 1995), our recent studies (Yao, 2000 and 2003; Yao and He 2003) show that a closed charge layer (CL) may provide a unique representation of the sources underneath the layer. And it may be utilized as an imaging of the underneath sources or as an approximate representation of the sources if they are actually located around the layer. Here we use the CL model to see if blurred alpha activity on the scalp can be segregated on the cortex. The details of the CL model are shown in the following appendix.

Methods

Eleven healthy right-handed male adult volunteers (age: 18-30 yrs.) were recruited from the university staff and students. Informed consent was obtained from each subject prior to the study. The study was approved by the Local Ethics Committee and made in accordance with the Helsinki Declaration. Each subject sat comfortably in a chair throughout the experiment in a quiet room (temperature at 20–21^{o}C). The head circumference of the subject, and the distance between the nasion and inion were measured. A suitable electro-cap was then used to record the EEG. The first electrode Fpz was 2 cm far from the nasion, and the Cz was located at the junction, halfway between the ears and the middle of the nasion and inion, when the cap was placed on the head. The ground electrode was placed halfway between the eyebrows. Electrodes M1 and M2 were placed on bilateral mastoids and were used as reference channels. Subjects were requested to relax and sit in a comfortable chair with their eyes closed. EEG recordings were carried out using 128-Channels high density A.N.T. System (0-550 Hz amplifier filter, 2048 Hz sampling frequency), including two electro-oculogram (EOG) channels and two reference channels M1 and M2. Ag/AgC1 electrodes (5 mm diameter) were attached to the scalp using electrode cream (EC2, Grass), and the electrode impedances were kept lower than 10 kΩ. The electrodes were mounted according to the montage 10-5 system (Oostenveld and Praamstra 2001). The EEG epochs of 2 minutes were sampled at 512 Hz. The on-line reference was the left mastoid, and the data were re-referenced off-line to average reference for further analysis.

In the CL inversion, as shown in figure 1, the head model is a four concentric spheres volume conductor (Cuffin and Cohen 1977). The radii were 7.9 cm, 8.1 cm, 8.5 cm, and 8.8 cm for the outer boundaries of the inner brain sphere, the cerebrospinal fluid layer, the skull layer, and the scalp layer, respectively. The conductivities are 0.461 $A(Vm)^{-1}$, 1.39 $A(Vm)^{-1}$, 0.0058 $A(Vm)^{-1}$, and 0.461 $A(Vm)^{-1}$, respectively. The discrete CL with 680 charges was set and uniformly distributed on an inner sphere surface with a radius of 7.5 cm. The CL estimation X was obtained by solving a linear equation V=GX where V is the scalp potential recordings, G is a matrix determined by the head volume conductor and the CL configuration on the layer. The inverse is computed by truncated singular value decomposition (SVD) pseudo-inverse (minimum norm solution), and the truncation is chosen at 31 where the ratio of the 31th singular value to the first singular value is 0.0178.

The scalp potentials V were segmented to epochs of 1 second, and epochs free of muscle, EOG, and movement artifacts were visually selected off-line. Both the inverted CL and scalp V were transformed by fast Fourier transform (FFT) to get the power (Welch's method in Matlab). For each subject, an Individual Alpha Peak Frequency (IAPF) of the power curves of the electrodes at O1 and O2 was identified, and the frequency band with IAPF ± 2 Hz was used to plot the power maps for the scalp and cortex CL, separately.

Results

In this study, the IAPF values at O1 and O2 for both the scalp potential and cortex CL are the same for ten of the eleven subjects: 11 Hz for four subjects, 10 Hz for five subjects, and 12 Hz for one. Only one subject has an 11 Hz IAPF on the scalp and 12Hz on the cortex. The results of three representative subjects are shown in figure 2. For the scalp

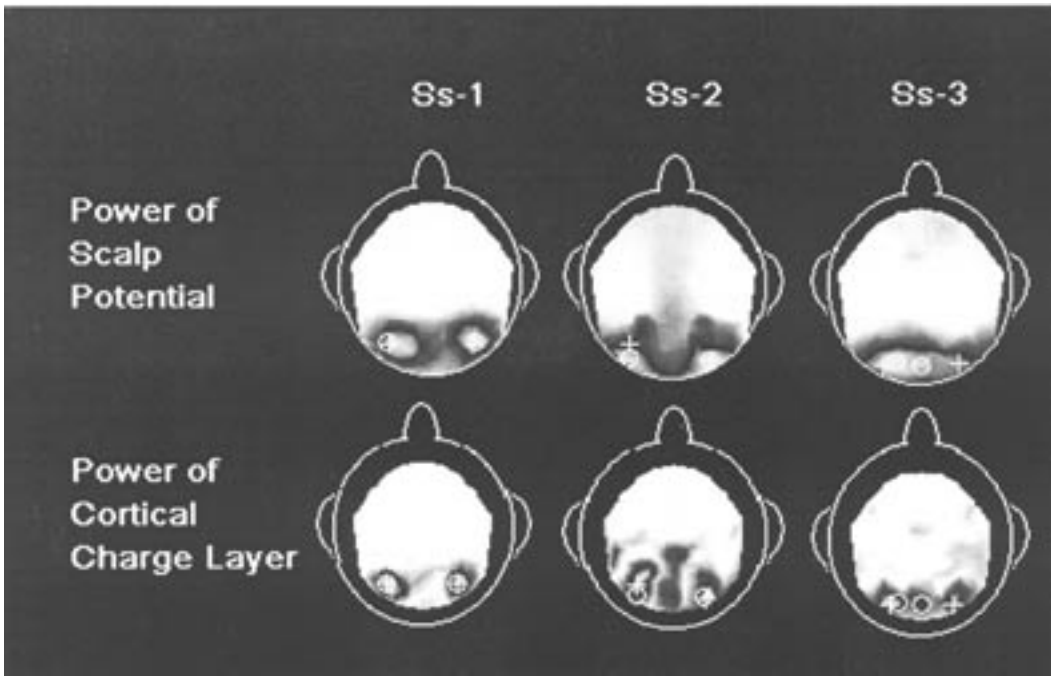

Figure 2. Normalized power maps of Alpha rhythms in frequency domain. The "o" and "+" indicate the left and right power maxima of the scalp potential and the cortex CL, respectively.

power map, seven of the eleven subjects show two distinctive occipital activities as Ss-1 and Ss-2 in figure 2. The other four cases show blurred occipital activities as Ss-3. However, for CL, all the maps of the eleven subjects clearly show a distinct location of the main activities at the left and right occipital regions. Seven CL maps of the eleven subjects have mainly two occipital activities as Ss-1, and the other four subjects have clearly sources located at the middle occipital region as Ss-2 and Ss-3. A parietal alpha, in addition to the occipital sites is also visible in the Ss-2.

Normalized spatial positions of the maxima and their spherical coordinates are shown in figure 3. They were searched automatically within each hemisphere. Based on figure 3, the maxima (+) of the cortex CL power are much more closer to each other (some of them are overlapped) than the maxima (o) of the scalp potential. The azimuth angles (radians) of the maxima positions are: -0.5±0.2 and 0.5±0.2 for the left and right scalp potential power, respectively, and -0.57±0.08 and 0.5±0.1 for the left and right cortex CL power, respectively. The elevation angles (radians) are: 0.3±0.1 for both the left and right scalp potential power, and 0.27±0.07 and 0.28±0.06 for the left and right cortex CL power, respectively. Paired statistic tests of the 11 subjects were conducted. The results show that the elevation angles between the left and right hemisphere for either the scalp potential or cortex CL, or between the scalp potential and the cortex CL for either the left or the right hemisphere are non-significant while the azimuth angles between the maxima positions of the left and right hemisphere are significantly ($p<0.001$) different for either the scalp potential or the cortex CL. The azimuth angles between the maxima positions of the scalp potential power and that of the cortex CL power for either the left or right hemisphere are also significantly ($p<0.05$) different. These results show that the local maximum of the scalp potential power is consistent in the elevation with that of the cortical CL power, and the maxima distributions between the scalp potential and the cortex CL are significantly different in azimuth as shown in figure 3.

About the frontal Alpha activities (Nunez et al. 2001), all our 11 subjects including the three in figure 2 did not show distinct frontal alpha activities. However, distinct IAPFs can be identified in ten of the eleven subjects at the normalized power spectra curves of the scalp potential at the electrodes positions F3 and F4, such as the three subjects shown in figure 4. This fact means that the frontal does have alpha electric activities (Nunez et al. 2001) though its strength is much smaller than the occipital region. While for the cortex CL, three F3 and five F4 (including Ss-1 and Ss-3 in figure 4) miss the IAPFs. Meanwhile, the IAPF values at F3 and F4 are the same as those at O1 and O2.

Discussions and Conclusion

When comparing with the scalp power mapping, the CL model is sensitive and able to segregate the

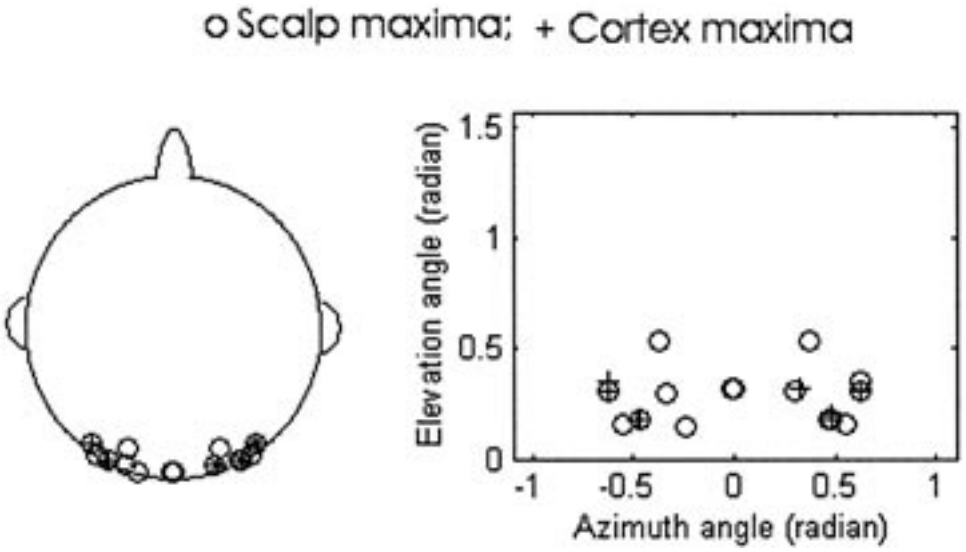

Figure 3. Normalized spatial positions of the maxima and their spherical coordinates. Left: normalized spatial positions of both the scalp potential power maxima (o) and the cortex CL power maxima. Right: the spherical coordinates of the maxima. For a Cartesian coordinate system with +x axis towards the right ear, y-axis towards the nasion, and +z axis towards the vertex, the azimuth angle is defined as the angle between the projection on xoy plane of a maxima point and the negative y-axis. A negative azimuth means the projection is in the –x direction. The elevation angle is defined as the angle between the maxima point and its projection on the xoy plane.

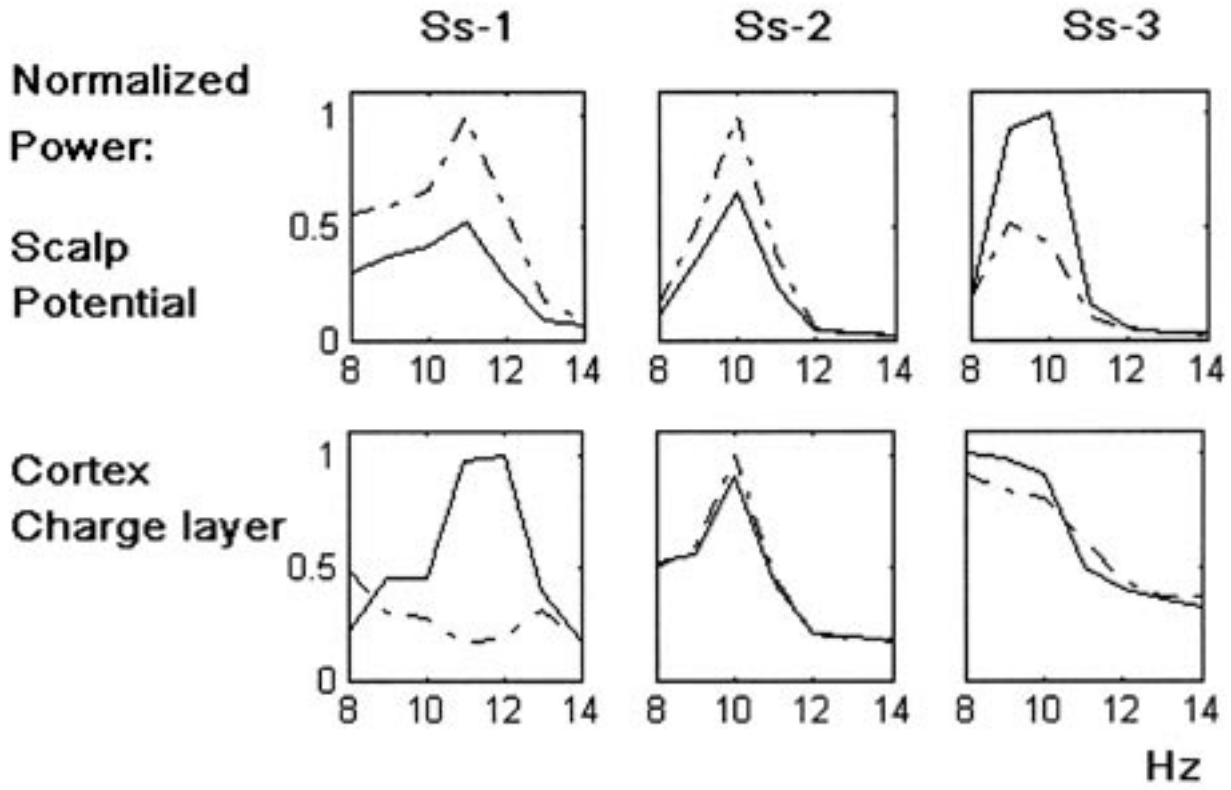

Figure 4. Normalized power spectra curves of scalp potential and cortex CL. The lateral axis is frequency (Hz). The spatial positions are F3 (solid line) and F4 (dashed line) on the scalp surface or cortex points with the same spherical coordinates.

blurred scalp activities into clear and separate regions at the cortex levels thus it provides more detailed information than the scalp power mapping. However, the distinct difference among the eleven subjects indicates various individual alpha generator pattern which means that a general conclusion of alpha generator needs to be based on many more subjects.

The CL imaging technique is based on the assumption that a closed CL can provide a unique representation of the source inside the layer, and it is this which tells us not to take the CL as the actual neural activities on the cortical surface in general, because this CL is the equivalent representation of all the sources on the layer and inside the layer. In fact, there is widespread evidence from intra-cranial recordings and fMRI studies that alpha rhythm generation involves sub-cortical and cortical structures (thalamus, insula) (Martinez-Montes et al. 2004). Meanwhile, though our results showed the alpha rhythm confined mainly to occipital and parietal areas, there are also some fMRI studies reporting alpha rhythm generators at the inferior frontal gyrus, cingulate areas and temporal cortex. How to integrate those various results from various imaging modalities remains a challenge topic.

Appendix

Equivalent Charge Model

In recent years, various imaging techniques have been developed (Yao 2000), such as the scalp Laplacian, cortical surface potential (CP) and the equivalent layer source imaging which consisted of two categories: equivalent dipole layer (DL) and equivalent charge layer (CL). Both DL and CL have been tested not only as an intermediate step to get CP (Sidman et al. 1992; Yao 1996) but also as an imaging quantity directly (Yao 2003). Our previous study shows that a distributed CL model may provide a higher spatial resolution than a distributed DL model does (Yao 2003), thus we chose the CL model to see if a blurred alpha activity on the scalp can be segregated on the cortex in this work.

As the equivalent charge model is not very popular, its rationale may be a concern. As the brain is a volume conductor, there is no static charge or dipole, but current in the tissues. For an active neuron in a conductive tissue, the total current $\vec{J}$ is consisted of two parts (Plonsey 1969; Malmivuo and Plonsey 1995): a primary (or driving) current flow $\vec{J}^P$ related to the original neural activity and a volume (or passive) current flow $\vec{J}^V$ that results from the effect of the electric field in the volume on extracellular charge carriers. $\vec{J} = \vec{J}^V + \vec{J}^P$. The primary current flows in the neuron and the volume current (secondary current) flows in the volume conductor (tissues). The two currents ($\vec{J}^P$ and $\vec{J}^V$) work together forming a closed current loop that makes the divergence of the total current $\vec{J}$ vanishes $\nabla \cdot \vec{J} = 0$ (Plonsey 1969; Malmivuo and Plonsey 1995), so there is no charge accumulation in a biological tissue that makes the net charge in any volume zero.

In general, the current is time-varying. As the change of the neural current is slow, a "quasi-static" approximation is commonly utilized in EEG and MEG practice (Plonsey 1969; Malmivuo and Plonsey 1995). For a stable-state current (quasi-static approximation), there is a duality rule between current field problem and the static electric field problem, this rule means that the current field $\vec{J}^V$, which is accessible by the body surface recordings, can be characterized by a scalar quantity – potential (Φ) governed by Possion's equation (Plonsey 1969; Malmivuo and Plonsey 1995)

$$\nabla^2 \Phi = \frac{\nabla \cdot \vec{J}^P}{\delta} = -\frac{I_V}{\delta} \qquad (1)$$

Where δ notes conductivity, and I_V is called "current source density (CSD)" (Mitzdorf and Singer, 1977). $\vec{J}$ ($\vec{J}^P$ and $\vec{J}^V$) is "current density (CD)" in strictly physical sense. Equation 1 shows that the current field ($\vec{J}^V$) or the potential (Φ) in the volume conductor is totally determined by the primary current density $\vec{J}^P$ (PCD) or I_V (CSD). Here for an illustration, considering PCD or CSD in a homogeneous volume conductor, we have(Plonsey 1969; Malmivuo and Plonsey 1995)

$$\Phi(\vec{r}) = \frac{1}{4\pi\delta} \int \vec{J}^P(\vec{r}') \cdot \frac{\vec{r} - \vec{r}'}{|\vec{r} - \vec{r}'|^3} d\vec{r}' \qquad (2)$$

Equation 2 shows that a segment of the primary current density $\vec{J}^P d\vec{r}'$ behaves like a dipole because it generates a field that varies as $1/r^2$, and a whole $\vec{J}^P$ behaves like a dipole distribution. Apparently, this fact provides a strong physical evidence for the dipole model used in biological electromagnetic field problem.

Meanwhile, according to equation 1, we have

$$\Phi(\vec{r}) = \frac{1}{4\pi\delta} \int \frac{\nabla \cdot \vec{J}^P(\vec{r}')}{|\vec{r} - \vec{r}'|} d\vec{r}' = \frac{1}{4\pi\delta} \int \frac{-I_v}{|\vec{r} - \vec{r}'|} d\vec{r}' \qquad (3)$$

Here CSD behaves like a charge because it generates a field that varies as *1/r*, so it provides a physical evidence of the equivalent charge model. It is the end point of the primary current, which flows in a neuron, i.e. the cell membrane where the current source density I_V appears.

In summary, the actual sources representing the neural electric activities are PCD or CSD, and the actual accessible physical quantity is the current field which arrives at the scalp surface, however, due to the duality rule between current field problem and the static electric

field problem (Plonsey 1969; Malmivuo and Plonsey 1995), their counterparts – the dipole, charge and potential are widely accepted in current practice of biological electric forward and inverse problem.

In practice, our main focus is the equivalent representation of the neural electric activities in the brain by physical charges or dipoles. The remaining question is the choice of them. In general, both of the charge model and dipole model are phenomenological description of the actual neuron electrical activities, so the choice depends on our concern. (1) The approximation of a model to the actual neural electric activities may be different on different spatial scale. For example, for an excited single neuron cell, both positive and negative (current source density) charges exist on its cell membrane (the surface of the cell body, axon and dendrites). When the spatial distance between a positive charge and a negative charge is large enough, a model with paired charges is a proper choice, otherwise, an integrated dipole formed by the paired positive and negative charges is a proper model. (2) The dipole model or charge model used in EEG inverse are in sense of macro scale average, and so the approximation also depends on the combination of neurons and shape of each neurons, for focal parallel small scale neurons combination, a dipole model may be the best; for parallel large scale neuron combination (with long dendrites and axon), a paired charges model may be a proper choice, and if the neurons are randomly distributed in a focal region, a quadrupole or even higher order model may be better than paired charges model or a dipole model. (3) The choice of source model also depends on the problem to solve, for example, if the model is utilized as a macro description of the actual focal neural electric activities, such as the case of EEG imaging, the conducted research shows that charge (scalar) source model is better than dipole (vector) source model in saving 2/3 of the unknowns (Yao and He 1998). If the model is utilized as an intermediate quantity to calculate other physical quantity such as the cortical surface potential, or as an imaging quantity such as the case shown here, the effectiveness depends on the uniqueness of the representation of the actual sources, and on practical feasibility including calculation and interpretation. The results shown in our previous works confirmed that CL may be used as an efficient imaging modality (Yao 2003) or as an intermediate step to get the cortical surface potential (Yao 1996 and 2000). (4) Based on the recent discussions of brain neural electric source model (Grave de Peralta et al. 2000), the basic biophysical relationship between the plausible generators and the measurements is

$$\Phi(\vec{r}) = \int \nabla\varphi(\vec{r}\,') \cdot \nabla G(\vec{r}, \vec{r}\,')d\vec{r}\,' = \int \nabla \cdot J^P G(\vec{r}, \vec{r}\,')d\vec{r}\,' = \int I_v G(\vec{r}, \vec{r}\,')d\vec{r}\,' \quad (3)$$

Where G is the Green function, and the $\varphi(\vec{r}\,')$, a variable proportional to the potential distribution within the brain, is assumed to be linked with the irrotational part of the primary current density, $(\vec{J}^P)_{\text{irrotational}} = \nabla\varphi(\vec{r}\,')$. Based on equation 3, the scalp potential doesn't contain information from the solenoidal part of $\vec{J}^P$, thus they proposed $\varphi(\vec{r}\,')$ as a restricted source model and specifically denoted it as ELECTRA (Grave de Peralta et al. 2000). Meanwhile, according to equation 3, I_V (equivalent charge model) is also linked to the irrotational part of $\vec{J}^P$ only. This fact means a charge (I_V) model is also a restricted source model than a dipole model. For a comparison between φ and I_V, both of them are scalar variables and an imaging method based on each one can reduce the number of unknowns to 1/3 of the general dipole case (Yao and He 1998; Grave de Peralta et al. 2000). Mathematically, we have

$$I_v = \nabla \cdot \vec{J}^P = \nabla \cdot \left\{ (\vec{J}^P)_{\text{solenoidal}} + (\vec{J}^P)_{\text{irrotational}} \right\} = \nabla \cdot (\vec{J}^P)_{\text{irrotational}} = \nabla^2 \varphi(\vec{r}\,') \quad (4)$$

here the difference between φ and I_V is only a Laplace operator and equation 4 looks like a Possion's equation where the charge is a physical source and the "potential" is the field of the physical source.

About the difference between the distributed source approach (CL and DL) and the dipole localization approaches (DLA) based on non-linear optimization algorithms, DLA may give a more concrete source location, however, it suffers from the instability inherent to the non-linear optimization. Meanwhile, CL or DL approach just results in an equivalent imaging map, and as the spatial positions of the assumed equivalent sources are assumed at first, the inversion is a much simpler linear inversion, and their results are unique in a sense of minimum norm constraint.

References

Adrian, E.D. and Matthews, B.H. The Berger rhythm: potential changes from the occipital lobes in man. Brain, 1934, 57: 355–385.

Basar, E., Schurmann, M., Basar-Eroglu, C. and Karakas, S. Alpha oscillations in brain functioning: an integrative theory. Int. J. of Psychophysiol., 1997, 26: 5-29.

Berger, H. ber das elektroenkephalogramm des menschen. Arch. Psychiat. Nervenkr., 1929, 87: 527–570.

Cuffin, B.N. and Cohen, D. Magnetic fields of a dipole in spherical volume conductor shapes. IEEE Trans. Biomed. Eng., 1977, 24: 372-381.

Grave de Peralta, R., Gonzalez Andino, S.L., Morand, S., Michel, C.M. and Landis, T. Imaging the electrical activity of the brain: ELECTRA. Human Brain Mapping, 2000, 9: 1-12.

Klimesch, W., Doppelmayr, M., Russegger, H., Pachinger, T.

and Schwaiger, J. Induced alpha band power changes in the human EEG and attention. Neuroscience Letters, 1998, 244: 73–76.

Lopes da Silva, F.H., Pijn, J.P., Velis, D. and Nijssen, P.C. Alpha rhythms: noise, dynamics and models. Int. J. Psychophysiol., 1997, 26: 237–249.

Lu, S.T., Kajola, M., Joutsiniemi, S.L., Knuutila, J. and Hari, R. Generator sites of spontaneous MEG activity during sleep. Electroenceph. Clin. Neurophysiol., 1992, 82: 182–196.

Malmivuo, J. and Plonsey, R. Bioelectromagnetism. Chapter 8. New York: Oxford University Press, 1995 (http://butler.cc.tut.fi/~malmivuo/bem/book/).

Martinez-Montes, E., Valdes-Sosa, P.A., Miwakeichi, F., Goldman, R.I and Cohen, M.S. Concurrent EEG/fMRI analysis by multiway Pprtial least squares. Neuroimage, 2004, 22:1023-1034.

Michel, C.M., Lehmann, D., Henggeler, B. and Brandeis D. Localization of the sources of EEG delta, theta, alpha and beta frequency bands using the FFT dipole approximation. Electroenceph. Clin. Neurophysiol., 1992, 82: 38-44.

Mitzdorf, U. and Singer, W. Laminar segregation of afferents to lateral geniculate nucleus of the cat: an analysis of current source density. J. Neurophysiol., 1977, 40: 1227–1244.

Narici, L. and Romani, G.L. Neuromagnetic investigation of synchronized spontaneous activity. Brain Topogr., 1989, 2: 19-30.

Niedermeyer, E. Alpha rhythms as physiological and abnormal phenomena. Int. J. Psychophsiol., 1997, 26: 31–49.

Nunez,P.L.,Wingeier,B.M. and Silberstein, R.B. Spatial-temporal structures of human alpha rhythms: theory, microcurrent sources, multiscale measurements, and global binding of local networks. Human Brain Mapping, 2001, 13: 125–164.

Parra, J., Meeren, H.K.M., Kalitzin, S., Suffczynskim, P., De Munck, J.C., Harding, G.F., Trenite, D.G. and Lopes da Silva, F.H. Magnetic source imaging in fixation-off sensitivity: relationship with alpha rhythm. J. Clin. Neurophysiol., 2000, 17: 212–223.

Patel, P., Khoslab, D., Al-Dayeha, L. and Singh, M. Distributed source imaging of alpha activity using a maximum entropy principle. Clin. Neurophysiol., 1999, 110: 538-549.

Perez-Borja, C., Chatrian, G.E., Tyce, F.A. and Rivers, M.H. Electrographic patterns of the occipital lobe in man: a topographic study based on use of implanted electrodes. Electroenceph. Clin. Neurophysiol., 1962, 14: 171-182.

Plonsey, R. Bioelectric Phenomena. New York: McGraw-Hill, 1969.

Rodin, E.A. and Rodin, M.J. Dipole sources of the human alpha rhythm. Brain Topogr., 1995, 7: 201-208.

Salenius, S., Kajola, M., Thompson, W.L., Kosslyn, S. and Hari, R. Reactivity of magnetic parieto-occipital alpha rhythm during visual imagery. Electroenceph. Clin. Neurophysiol., 1995, 95: 453–462.

Sidman, R.D., Vincent, D.J., Smith, D.B. and Lee, L. Experimental tests of the cortical imaging technique IEEE Trans Biomed. Eng., 1992, 39: 437–444.

Tesche, C. and Kajola, M. A comparison of the localization of spontaneous neuromagnetic activity in the frequency and time domains. Electroenceph. Clin. Neurophysiol. 1993; 87: 408-416.

Tesche, C.D., Uusitalo, M.A., Ilmoniemi, R.J., Huotilainen, M., Kajola, M. and Salonen, O. Signal-space projections of MEG data characterize both distributed and well-localized neuronal sources. Electroenceph. Clin. Neurophysiol., 1995, 95: 189-200.

Williamson, S. and Kaufman, L. Advances in neuromagnetic instrumentation and studies of spontaneous brain activity. Brain Topogr., 1989, 2: 129–139.

Yao, D. The equivalent source technique and cortical imaging. Electroenceph. Clin. Neurophysiol., 1996, 98: 478–483.

Yao, D. and He, B. The Laplacian weighted minimum estimate of three dimensional equivalent charge distribution in the brain. Proc IEEE-EMBS, 1998, 20: 2108-2111.

Yao, D. High-resolution EEG mappings: a spherical harmonic spectra theory and simulation results. Clin. Neurophysiol., 2000, 111: 81-92.

Yao, D. High-resolution EEG mapping: an equivalent charge-layer approach. Physics In Medicine and Biology, 2003, 48: 1997-2011.

Yao, D. and He, B. Equivalent physical models and formulation of equivalent source layer in high-resolution EEG imaging. Physics in Medicine and Biology, 2003, 48: 3475-3483.